




ClampFISH detects individual nucleic acid molecules using click chemistry–based amplification

Sara H Rouhanifard¹ , Ian A Mellis^{1,2} , Margaret Dunagin¹, Sareh Bayatpour¹, Connie L Jiang^{1,3}, Ian Dardani¹, Orsolya Symmons¹, Benjamin Emert^{1,2}, Eduardo Torre^{1,4}, Allison Cote¹, Alessandra Sullivan⁵, John A Stamatoyannopoulos⁵ & Arjun Raj^{1,2,6} 

Methods for detecting single nucleic acids in cell and tissues, such as fluorescence *in situ* hybridization (FISH), are limited by relatively low signal intensity and nonspecific probe binding. Here we present click-amplifying FISH (clampFISH), a method for fluorescence detection of nucleic acids that achieves high specificity and high-gain (>400-fold) signal amplification. ClampFISH probes form a ‘C’ configuration upon hybridization to the sequence of interest in a double helical manner. The ends of the probes are ligated together using bio-orthogonal click chemistry, effectively locking the probes around the target. Iterative rounds of hybridization and click amplify the fluorescence intensity. We show that clampFISH enables the detection of RNA species with low-magnification microscopy and in RNA-based flow cytometry. Additionally, we show that the modular design of clampFISH probes allows multiplexing of RNA and DNA detection, that the locking mechanism prevents probe detachment in expansion microscopy, and that clampFISH can be applied in tissue samples.

Single-molecule RNA fluorescence *in situ* hybridization (RNA FISH), which enables the direct detection of individual RNA molecules^{1–3}, has emerged as a powerful technique for measuring both RNA abundance and localization in single cells. Yet, while single-molecule RNA FISH is simple and robust, the total signal generated by single-molecule RNA FISH probes is low, thus requiring high-powered microscopy for detection. This keeps throughput relatively low and precludes the use of downstream detection methods such as flow cytometry. As such, amplification methods for single-molecule RNA FISH with high efficiency, specificity and gain could enable many new applications.

A number of signal amplification techniques are available, but each suffers from particular limitations due to dependence on enzymatic activity or hybridization alone for signal gain. Approaches such as tyramide signal amplification⁴ or enzyme-ligated fluorescence⁵ utilize enzymes to catalyze the deposition of fluorescent substrates near the probes. Alternatively, in techniques such as rolling-circle amplification, enzymes ligate oligonucleotides to form a circular probe and

then catalyze a ‘rolling-circle’ nucleic acid amplification to generate a repeating sequence, which can be detected using fluorescent oligonucleotides^{6–8}. These methods can lead to large signal gains, but are limited by the accessibility of (sometimes multiple) bulky enzymes that need to diffuse through the fixed cellular environment to reach their target molecules. For example, the DNA ligases frequently used to circularize ‘padlock’ probes are often quite inefficient⁹, contributing to inconsistent amplification¹⁰.

Nonenzymatic amplification schemes, most notably the hybridization chain reaction^{11–13} and branched DNA^{14–16} techniques, rely only on hybridization to amplify signal. However, their larger DNA scaffolds, to which fluorescent probes attach, often have limited amplification potential¹⁷ and generally lack assay design flexibility for multiplexing. Thus, our goal was to create a nonenzymatic, exponential amplification scheme with high sensitivity (detection efficiency), very high gain (signal amplification), and specificity (low background).

We first designed probes that would bind with high specificity and sensitivity; i.e., that could allow the probes to survive repeated liquid handling in conditions stringent enough to limit nonspecific binding and thus prevent spurious amplification. Padlock probes are a class of circular DNA probes that have these properties: they bind to the target region of complementarity via the 5′ and 3′ ends of the probe, with the intervening sequence, not hybridized to the target, in a ‘C’ configuration¹⁸. Conventionally, the ends are then connected using a DNA or RNA¹⁹ ligase. This connection, in combination with the DNA:RNA double helix formed upon hybridization, result in a molecule that is physically wrapped around the target strand (**Fig. 1a**). We wished to retain the benefits of padlock probes without the need for this enzymatic ligation; therefore, we designed padlock-style probes with terminal alkyne and azide moieties at the 5′ and 3′ ends, termed click-amplifying FISH (clampFISH) probes (**Fig. 1a** and **Supplementary Fig. 1**). When the clampFISH probe hybridizes to the target RNA, the DNA:RNA hybrid brings the two moieties together in physical space. We then used a click chemistry strategy (copper(I)-catalyzed azide–alkyne cycloaddition, CuAAC²⁰) to covalently link

¹Department of Bioengineering, University of Pennsylvania, Philadelphia Pennsylvania, USA. ²Genomics and Computational Biology Group, Perelman School of Medicine, University of Pennsylvania, Philadelphia, Pennsylvania, USA. ³Cell and Molecular Biology Group, Perelman School of Medicine, University of Pennsylvania, Philadelphia, Pennsylvania, USA. ⁴Department of Biochemistry and Biophysics, Perelman School of Medicine, University of Pennsylvania, Philadelphia, Pennsylvania, USA. ⁵Altius Institute for Biomedical Sciences, Seattle, Washington, USA. ⁶Department of Genetics, Perelman School of Medicine, University of Pennsylvania, Philadelphia, Pennsylvania, USA. Correspondence should be addressed to A.R. (arjunrajlab@gmail.com).

Received 7 May; accepted 24 September; published online 12 November 2018; doi:10.1038/nbt.4286

the 5'-alkyne and 3'-azide ends of the probe, effectively forming a loop around the target RNA (Fig. 1a).

To achieve exponential amplification, we first designed a series of primary clampFISH probes to target the RNA sequence of interest. The backbone of each primary clampFISH probe contains two 'landing pads' for a set of secondary, fluorescent clampFISH probes. The number of landing pads may be modified to increase amplification (Supplementary Fig. 1). To the backbones of these secondary probes, we hybridized a set of tertiary probes that bind in a 2:1 ratio. In a subsequent round, the secondary probes again bind 2:1 to the backbones of tertiary probes and so on, thereby in principle doubling the signal in each round (Fig. 1b). The resulting probes bound efficiently to the target, as evidenced by the colocalization of clampFISH probes with single-molecule RNA FISH probes targeting the same RNA (Fig. 1c and Supplementary Fig. 2). We observed that many non-colocalizing spots often corresponded to faint single-molecule FISH spots that were not picked up by our thresholding software for single-molecule FISH. The absence of clampFISH spots in our genetic negative controls suggests that these faint spots may in fact be true positive signal. The number of amplification rounds may be adjusted according to the desired degree of amplification required for the particular application (Fig. 1d).

To demonstrate exponential amplification using clampFISH probes, we first targeted and amplified *GFP* mRNA in a human melanoma cell line (WM983b) stably expressing GFP²¹ using a set of ten primary clampFISH probes (Fig. 1e). We used stringent hybridization conditions—specifically, a higher concentration of formamide than is traditionally used for single-molecule RNA FISH—to limit nonspecific probe binding while still allowing specific binding (Supplementary Fig. 3). As the number of rounds progressed, the average number of spots per cell remained constant (for example, at round 2 we detected a mean of 399 spots per cell \pm 62 s.e.m. and at round 10 we detected 401 spots per cell \pm 36; Fig. 1f), while the intensity of the signal as measured by fluorescence microscopy increased. At round 12, the mean signal per spot was 446-fold higher than in round 2 (Fig. 1i). We observed a 3.39-fold \pm 1.29 increase (geometric mean and geometric s.d. of fold changes in average spot intensity in two-round intervals from rounds 2–12) for every two rounds of amplification (for an average 1.69-fold increase per round; Fig. 1g–i). We also observed that the fold amplification decreased slightly at later rounds, and we estimate that the saturation point—i.e., the estimated point at which no further amplification would occur—would be reached around round 20 (Supplementary Fig. 4).

To assess whether the click reaction aided in the amplification process as hypothesized, we performed the same experiment in the absence of the click ligation of the clampFISH probes. Although the number of spots detected per cell was similar (393 mean spots per cell in the clicked samples vs. 381 mean spots per cell in the non-clicked samples), we observed lower mean signal intensity (26,076 arbitrary units (AU) \pm 496 for non-clicked vs. 44,450 AU \pm 630 for clicked samples at round 12), as well as a lack of uniformity in spot intensity (coefficient of variation at round 12 for non-clicked samples 0.94 \pm 0.013, vs. 0.69 \pm 0.01 for clicked samples), demonstrating that the click reaction facilitated a more uniform and higher gain amplification of clampFISH signal (Fig. 1h and Supplementary Fig. 5).

To demonstrate signal specificity, we performed the same clampFISH detection and amplification on the parental cell line that did not have the *GFP* gene. We detected very few false-positive spots in these cells (mean of 9.77 spots per cell \pm 1.45), showing that the signals were specific to the target (Fig. 1e). Although this number is low, it may interfere with the detection of RNAs with few transcripts per cell.

Owing to its relatively low signal intensity, single-molecule RNA FISH typically requires using a microscope equipped with a high-numerical-aperture oil immersion objective. For many applications, a low-magnification air objective is preferable, both for increased throughput and for simplicity of sample handling. We reasoned that the increased signals that clampFISH provided could make RNA FISH signals detectable by low-magnification microscopy (Fig. 2a). To test this, we mixed 20% WM983b cells stably expressing GFP with 80% WM983b cells without GFP and probed for *GFP* mRNA using clampFISH probes at round 6—this was the minimum number of rounds needed to clearly discern signal at the lowest magnification for this particular target. Using clampFISH, the positive cells were clearly discernible at both 20 \times and 10 \times magnification, whereas the conventional single-molecule RNA FISH signal was not (Fig. 2a). To demonstrate the speed of image acquisition for high-throughput applications, we applied clampFISH to detect *HIST1H4E*, an RNA target lacking a corresponding antibody for detection (Fig. 2b and Supplementary Fig. 6). Scanning one well of a 96-well plate took \sim 21 min at 20 \times magnification using clampFISH, as opposed to \sim 4 h at 60 \times magnification using single-molecule RNA FISH.

Primary tissue samples typically suffer from high background levels that contribute to a low signal-to-noise ratio using single-molecule RNA FISH and therefore require high-magnification microscopy to distinguish positive signal from background. However, at high magnification, large structural features of the tissue are often difficult to discern, and tiled image scanning is relatively slow. To increase the field of view while still imaging individual RNAs, we applied four rounds of clampFISH to kidney samples from 4-day-old C57BL/6J mice and probed for *Podxl* mRNA, which is highly expressed in podocytes²², and observed specific clampFISH signal in the appropriate regions (Fig. 2c and Supplementary Fig. 7). ClampFISH further revealed *Podxl* to be expressed in the kidney endothelium as well, a signal that was only faintly visible by single-molecule RNA FISH but was clearly detected by clampFISH at low magnification (Fig. 2c). This is consistent with previous findings that *Podxl* is expressed at low levels in the kidney endothelium²³ and highlights the utility of clampFISH for detection of low-abundance transcripts in tissue.

Another application that clampFISH enables is flow-cytometry-based measurement of RNA expression, an application for which single-molecule RNA FISH typically does not produce enough signal^{24,25}. We applied clampFISH to a mixed population of MDA-MB-231 cells with and without GFP expression and analyzed the cells by flow cytometry (Fig. 2d and Supplementary Figs. 8 and 9), using GFP fluorescence as an independent measure of the specificity of clampFISH signal. We observed separation of GFP-positive cells by clampFISH signal with as few as two rounds of amplification, and observed a 2.447-fold increase in fluorescence intensity in the GFP-positive population with every two rounds of amplification thereafter (geometric mean of fold change across rounds; Fig. 2d and Supplementary Fig. 8). Notably, we observed a decreasing fold-change as we moved through the rounds (3.435-fold from rounds 2–4, 2.589-fold from rounds 4–6, and 1.648-fold from rounds 6–8). We also used clampFISH to sort cells on the basis of endogenous RNA expression for *HIST1H4E* mRNA and the long noncoding RNA (lncRNA) *NEAT1* (Fig. 2e), relatively low abundance targets that cannot be detected using antibodies.

Amplification of RNA signal can also be used in combination with a newly developed expansion microscopy technique that achieves super-resolution microscopy via the physical expansion of cells embedded in polymeric hydrogels^{26,27}. When combined with single-molecule RNA FISH, expansion microscopy can resolve the fine structure of

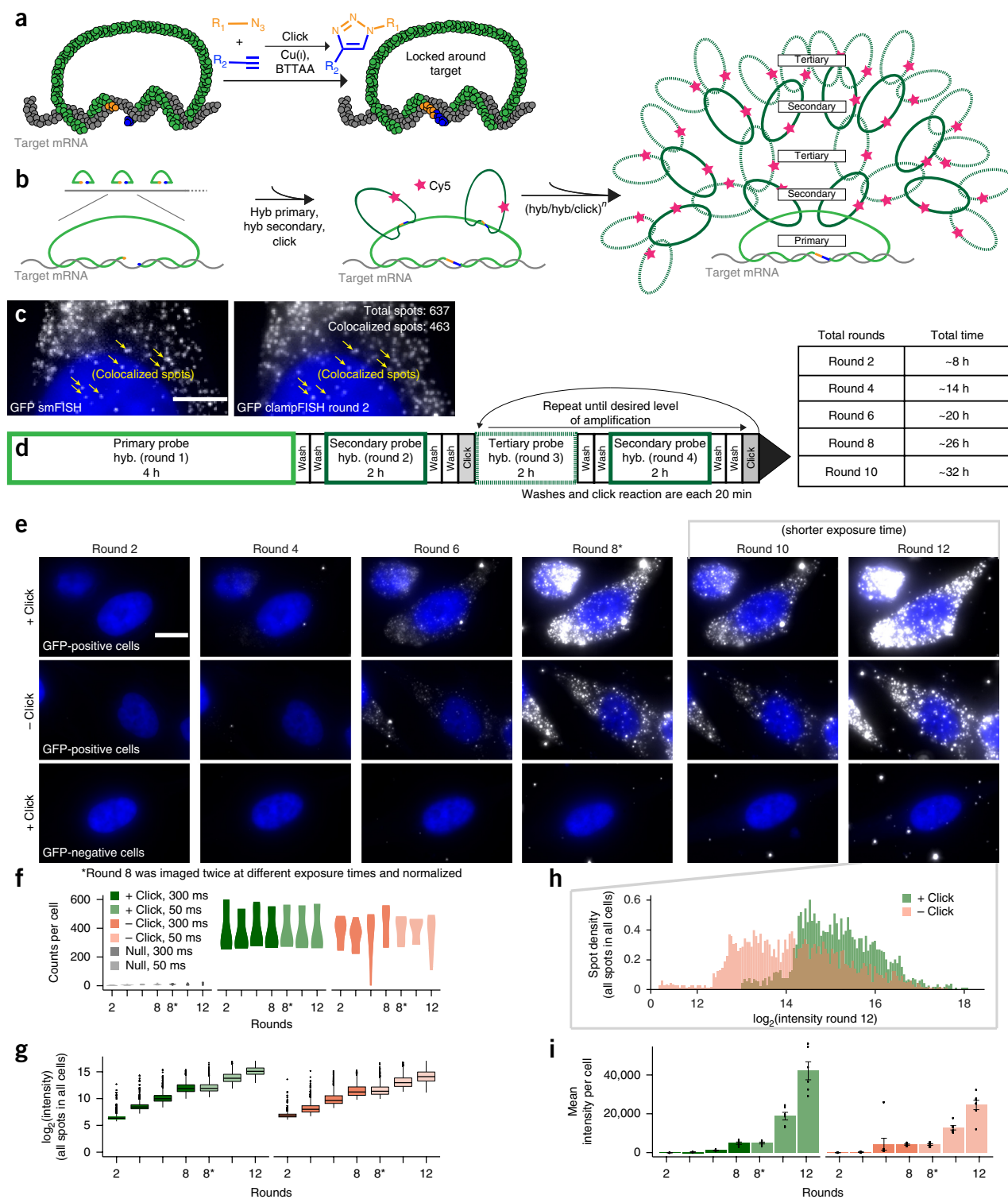


Figure 1 Design and validation of clampFISH technology. **(a)** Schematic of clampFISH probe binding and ligation using CuAAC. **(b)** ClampFISH workflow for doubling fluorescent signal at every round of hybridization (hyb). **(c)** Colocalization of *GFP* mRNA single-molecule RNA FISH signal (left) with *GFP* mRNA clampFISH signal at round 2 (right; scale bar, 5 μ m). **(d)** Timing and order of clampFISH amplification steps. **(e)** *GFP* mRNA clampFISH signal on WM983b-GFP cells across 12 rounds of amplification in the presence of click ligation (top) compared to *GFP* mRNA clampFISH signal in the absence of click ligation (middle). Bottom, single-cell tracking of the same cell line without *GFP* mRNA expression across rounds (scale bar, 10 μ m). Images are representative single cells selected from three independent experiments. **(f)** mRNA counts per cells across 12 rounds of amplification. **(g)** \log_2 (intensity) of click vs. no-click samples across 12 rounds of amplification. Center line, median \log_2 (intensity); box limits, first and third quartile \log_2 (intensity) values; whiskers, observations within 1.5 \times the interquartile range of the box limits. **(h)** Density of the \log_2 (intensity) of all spots detected at round 12 in click vs. no-click samples. **(i)** Mean fluorescence intensity of *GFP* mRNA clampFISH signal per cell on WM983b-GFP cells across 12 rounds of clampFISH. All graphs are representative of three independent experiments.

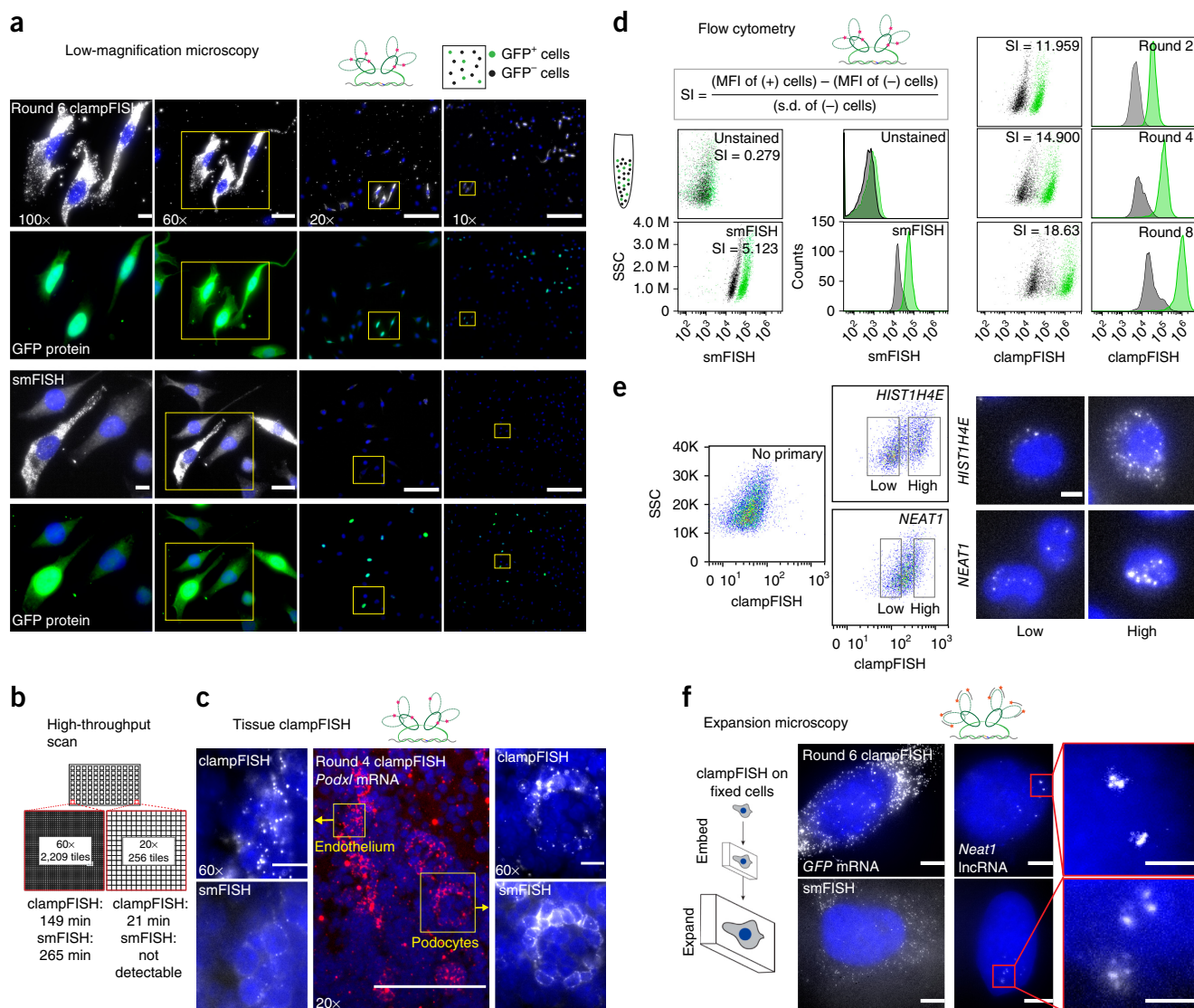


Figure 2 Applications of clampFISH amplification of RNA. **(a)** ClampFISH applied to detect *GFP* mRNA in a mixed population of WM983b cells and WM983b cells stably expressing GFP (top) and compared to *GFP* single-molecule FISH (smFISH, bottom) using 0.3 NA 10×, 0.5 NA 20×, 1.4 NA 60× and 1.4 NA 100× objectives (representative images from two independent experiments; each image is contrasted independently; scale bars are 10 μm for 100× and 60×, 5 μm for 20× and 2.5 μm for 10×). Each image has a corresponding image showing *GFP* mRNA signal colocalizing with GFP protein. **(b)** Speed of image acquisition for a scan of an individual well from a 96-well plate equivalent. clampFISH at round 6 is compared to smFISH with 20× and 60× objectives. **(c)** Center, 20× image of fixed and frozen 5-μm kidney section from a 4-d-old mouse stained with round 4 clampFISH probes targeting *Podxl*. Left, 60× image of mouse kidney endothelium by round 4 clampFISH and by single-molecule RNA FISH. Right, 60× image of podocyte by round 4 clampFISH and by single-molecule RNA FISH (representative images shown from two independent experiments). Scale bars are 5 μm for 60× and 20× images. **(d)** clampFISH was applied to a mixed population of MDA-MB-231 cells with and without GFP expression and analyzed by flow cytometry across eight rounds of amplification. Cells were gated on *GFP* expression and are displayed in green; cells without GFP expression are displayed in black. SI, staining index; SSC, side scatter; MFI, mean fluorescence intensity. **(e)** Flow cytometric plots (pseudocolored) showing gating strategy for *HIST1H4E* mRNA and *NEAT1* lncRNA expression on HeLa cells after six rounds of amplification. High and low expressers were sorted and imaged by fluorescence microscopy (scale bar, 20 μm). **(f)** Top, fluorescence micrographs of round 6 clampFISH targeting *GFP* mRNA and *NEAT1* lncRNA in cultured WM983b-GFP cells (bottom) fluorescence micrographs of single-molecule RNA FISH targeting *GFP* mRNA and *NEAT1* lncRNA in cultured WM983b-GFP cells using the same dye (images representative of two independent experiments; scale bars are 20 μm for the main images and 5 μm for the insets).

RNAs that are in close proximity to one another; however, the physical expansion of cells results in reduced signal intensities, at least partially as a result of probes dissociating under the low-salt conditions required to obtain high levels of hydrogel expansion. We reasoned that the locking property of clampFISH probes would allow us to maintain signal intensity in the face of these expansion conditions. We thus

performed clampFISH on *GFP* mRNA to round 6, followed by expansion, and observed high signal intensity on all spots when the click reaction was performed, but little signal when click was not performed (**Fig. 2d** and **Supplementary Fig. 10**). We also applied clampFISH to amplify *NEAT1*, a nuclear retained lncRNA, to round 6 and observed higher signal intensity than with single-molecule RNA FISH (**Fig. 2d**

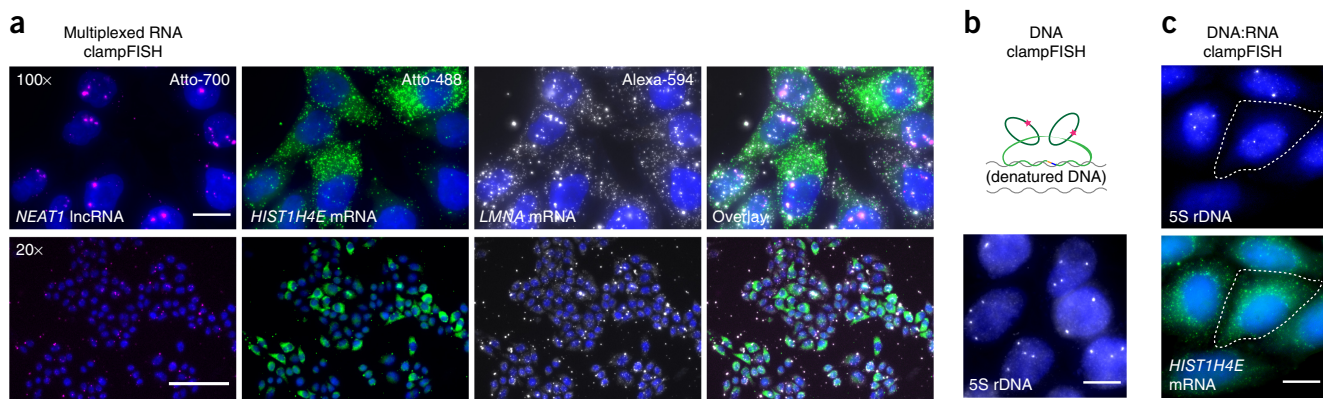


Figure 3 Multiplexing of amplified RNA and DNA targets. **(a)** Fluorescent micrographs of individual probe channels: from left, *NEAT1* IncRNA labeled with Atto 700, *HIST1H4E* mRNA labeled with Atto 488, and *LMNA* mRNA labeled with Alexa 594, and an overlay at far right. Top, 100 \times objective with 20- μ m scale bars; bottom, 20 \times objective with 20- μ m scale bars. Images are representative of two independent experiments. **(b)** DNA clampFISH of 5S rDNA was performed to two rounds on HeLa cells and detected using Cy5. Scale bar, 20 μ m. **(c)** Multiplexed DNA and RNA clampFISH of *HIST1H4E* and DNA clampFISH of 5S rDNA in HeLa cells. Scale bar, 20 μ m.

and **Supplementary Fig. 10**). This also suggests that the nucleus is accessible to clampFISH probes, which can be a problem with other amplification schemes¹⁶. Notably, we also observed nuclear localization of the *GFP* mRNA using clampFISH probes (**Fig. 1c,e**), but did not detect transcription sites. Upon further analysis, we determined that clampFISH probes can enter the nucleus but may have difficulty accessing transcription sites (data not shown), possibly as a result of crowding from RNA secondary structure or nearby proteins.

A key design goal for FISH methods is the ability to detect multiple RNA targets simultaneously. Multiplexing with clampFISH is in principle straightforward because of the modular design of the probes. The backbone sequence of the clampFISH probes can easily be changed, allowing one to use multiple independent amplifiers simultaneously. Many transcripts may be amplified simultaneously with unique backbone sequences that are not labeled with a fluorophore, and the subsequent loop-dendrimer structure can be probed with fluorescently labeled secondary fluorescent oligonucleotides that can be easily removed and rehybridized. As a proof of concept, we selected three RNA targets with distinct expression patterns in HeLa cells: *NEAT1*, which is found in nuclear paraspeckles of most cells; *LMNA*, which is found in the cytoplasm of all cells, and *HIST1H4E*, which is expressed only in the subpopulation of cells that are in S phase. We amplified these with unique sets of nonfluorescent clampFISH probes to seven rounds and then probed the terminal backbones with single-molecule RNA FISH probes, each labeled with different fluorophores (**Fig. 3a** and **Supplementary Fig. 11**). We were able to visualize signals from the three different probe sets, even using low-magnification microscopy. We observed that *LMNA* was present in nuclear paraspeckles and therefore colocalized with the *NEAT1* signal. We confirmed that this was not bleedthrough by imaging each probe, amplified to seven rounds in every channel, using the same exposure times and observing no signal in the off-channels (**Supplementary Fig. 11**).

Our method for the amplification of fluorescent RNA signals *in situ* is different from other nonenzymatic, hybridization-based technologies because it directly links the probe to the target RNA whereas other systems are susceptible to probe detachment during washes. In a direct comparison with commercially available systems, we observed that other methods' maximum fluorescence intensity

amplification was comparable to that of clampFISH at six rounds (**Supplementary Fig. 12**); however, the fluorescence intensity of clampFISH far surpassed other methods beyond round 6. Thus, the clampFISH amplification system can enable assays that require extremely high signal gain, especially flow cytometry (**Fig. 2c**) and high-throughput microscopy of targets with lower expression levels (**Fig. 3a**). For instance, we were able to detect *HIST1H4E* RNA with low-power microscopy even though it is typically expressed at levels of only around 200 molecules per cell²¹ (**Fig. 3a**).

Further benefits of clampFISH include tunable, exponential amplification of fluorescence intensity (**Fig. 1**), modular probe design for simplified and expanded multiplexing capabilities, and compatibility with expansion microscopy. Notably, the ends of the clampFISH probes behave as a proximity ligation wherein the click reaction will occur if and only if the two arms are hybridized adjacent to each other (**Supplementary Fig. 13**), suggesting that clampFISH may find uses in specifically probing RNA subsets such as splicing junctions, short alternatively spliced variants, or edited RNAs. Finally, we applied a modified clampFISH hybridization scheme to detect 5S rDNA²⁸ loci in single cells (**Fig. 3b** and **Supplementary Fig. 14**). When we performed *HIST1H4E* RNA clampFISH before 5S rDNA clampFISH, we found that the probes can survive these steps and enable simultaneous amplification and imaging of both DNA and RNA (**Fig. 3c** and **Supplementary Fig. 14**). The stringent hybridization conditions of DNA FISH are not typically compatible with RNA FISH.

METHODS

Methods, including statements of data availability and any associated accession codes and references, are available in the [online version of the paper](#).

Note: Any Supplementary Information and Source Data files are available in the online version of the paper.

ACKNOWLEDGMENTS

We thank F. Tuluc from the CHOP flow cytometry core facility for discussions and assistance with flow cytometry. We also thank J. Peterson for his early contributions and the many bioRxiv readers who reached out with feedback and suggestions. S.H.R. acknowledges support from NIH 1F32GM120929-01A1; I.A.M. acknowledges support from NIH F30 NS100595; O.S. acknowledges support from the Human Frontier Science Program LT000919/2016-1; C.L.J. acknowledges support from NIH 5T32DK007780-19; and A.R. from NIH 4DN U01 HL129998,

NIH Center for Photogenomics RM1 HG007743, the Chan Zuckerberg Initiative and HCA Pilot Project 174285, NSF CAREER 1350601 and NIH R33 EB019767.

AUTHOR CONTRIBUTIONS

S.H.R. and A.R. designed the study and wrote the manuscript. I.A.M. performed statistical analysis. S.H.R., M.D., S.B., C.L.J., I.D., O.S., B.E., E.T., A.C., A.S. and J.A.S. designed and performed the experiments.

COMPETING INTERESTS

A.R. receives royalties related to Stellaris RNA FISH probes.

Reprints and permissions information is available online at <http://www.nature.com/reprints/index.html>. Publisher's note: Springer Nature remains neutral with regard to jurisdictional claims in published maps and institutional affiliations.

- Femino, A.M., Fay, F.S., Fogarty, K. & Singer, R.H. Visualization of single RNA transcripts in situ. *Science* **280**, 585–590 (1998).
- Raj, A., van den Bogaard, P., Rifkin, S.A., van Oudenaarden, A. & Tyagi, S. Imaging individual mRNA molecules using multiple singly labeled probes. *Nat. Methods* **5**, 877–879 (2008).
- Itzkovitz, S. & van Oudenaarden, A. Validating transcripts with probes and imaging technology. *Nat. Methods* **8**(Suppl.), S12–S19 (2011).
- Chen, C.H. *et al.* Specific sorting of single bacterial cells with microfabricated fluorescence-activated cell sorting and tyramide signal amplification fluorescence in situ hybridization. *Anal. Chem.* **83**, 7269–7275 (2011).
- Lu, J. & Tsourkas, A. Imaging individual microRNAs in single mammalian cells in situ. *Nucleic Acids Res.* **37**, e100 (2009).
- Banér, J., Nilsson, M., Mendel-Hartvig, M. & Landegren, U. Signal amplification of padlock probes by rolling circle replication. *Nucleic Acids Res.* **26**, 5073–5078 (1998).
- Larsson, C., Grundberg, I., Söderberg, O. & Nilsson, M. In situ detection and genotyping of individual mRNA molecules. *Nat. Methods* **7**, 395–397 (2010).
- Ali, M.M. *et al.* Rolling circle amplification: a versatile tool for chemical biology, materials science and medicine. *Chem. Soc. Rev.* **43**, 3324–3341 (2014).
- Lohman, G.J.S., Zhang, Y., Zhelkovsky, A.M., Cantor, E.J. & Evans, T.C. Jr. Efficient DNA ligation in DNA-RNA hybrid helices by Chlorella virus DNA ligase. *Nucleic Acids Res.* **42**, 1831–1844 (2014).
- Lagunavicius, A. *et al.* Novel application of Phi29 DNA polymerase: RNA detection and analysis in vitro and in situ by target RNA-primed RCA. *RNA* **15**, 765–771 (2009).
- Dirks, R.M. & Pierce, N.A. Triggered amplification by hybridization chain reaction. *Proc. Natl. Acad. Sci. USA* **101**, 15275–15278 (2004).
- Choi, H.M.T., Beck, V.A. & Pierce, N.A. Next-generation in situ hybridization chain reaction: higher gain, lower cost, greater durability. *ACS Nano* **8**, 4284–4294 (2014).
- Shah, S. *et al.* Single-molecule RNA detection at depth via hybridization chain reaction and tissue hydrogel embedding and clearing. *Development* **143**, 2862–2867 (2016).
- Lau, J.Y. *et al.* Significance of serum hepatitis C virus RNA levels in chronic hepatitis C. *Lancet* **341**, 1501–1504 (1993).
- Kern, D. *et al.* An enhanced-sensitivity branched-DNA assay for quantification of human immunodeficiency virus type 1 RNA in plasma. *J. Clin. Microbiol.* **34**, 3196–3202 (1996).
- Battich, N., Stoeger, T. & Pelkmans, L. Image-based transcriptomics in thousands of single human cells at single-molecule resolution. *Nat. Methods* **10**, 1127–1133 (2013).
- Shah, S. *et al.* Single-molecule RNA detection at depth by hybridization chain reaction and tissue hydrogel embedding and clearing. *Development* **143**, 2862–2867 (2016).
- Nilsson, M. *et al.* Padlock probes: circularizing oligonucleotides for localized DNA detection. *Science* **265**, 2085–2088 (1994).
- Jin, J., Vaud, S., Zhelkovsky, A.M., Posfai, J. & McReynolds, L.A. Sensitive and specific miRNA detection method using SplintR ligase. *Nucleic Acids Res.* **44**, e116 (2016).
- Besanceney-Webler, C. *et al.* Increasing the efficacy of bioorthogonal click reactions for bioconjugation: a comparative study. *Angew. Chem. Int. Edn. Engl.* **50**, 8051–8056 (2011).
- Padovan-Merhar, O. *et al.* Single mammalian cells compensate for differences in cellular volume and DNA copy number through independent global transcriptional mechanisms. *Mol. Cell* **58**, 339–352 (2015).
- Kerjaschki, D., Sharkey, D.J. & Farquhar, M.G. Identification and characterization of podocalyxin—the major sialoprotein of the renal glomerular epithelial cell. *J. Cell Biol.* **98**, 1591–1596 (1984).
- Horrillo, A., Porras, G., Ayuso, M.S. & González-Manchón, C. Loss of endothelial barrier integrity in mice with conditional ablation of podocalyxin (Podxl) in endothelial cells. *Eur. J. Cell Biol.* **95**, 265–276 (2016).
- Klemm, S. *et al.* Transcriptional profiling of cells sorted by RNA abundance. *Nat. Methods* **11**, 549–551 (2014).
- Bushkin, Y. *et al.* Profiling T cell activation using single-molecule fluorescence in situ hybridization and flow cytometry. *J. Immunol.* **194**, 836–841 (2015).
- Chen, F., Tillberg, P.W. & Boyden, E.S. Expansion microscopy. *Science* **347**, 543–548 (2015).
- Chen, F. *et al.* Nanoscale imaging of RNA with expansion microscopy. *Nat. Methods* **13**, 679–684 (2016).
- Pelliccia, F., Gaddini, L., Limongi, M.Z. & Rocchi, A. Visualizing human 5S rDNA. *Chromosome Res.* **5**, 205–207 (1997).

ONLINE METHODS

Cell culture. We cultured WM983b cells and WM983b-GFP-NLS cells (a human metastatic melanoma cell line from the laboratory of M. Herlyn at The Wistar Institute) in tumor specialized medium containing 2% FBS. The WM983b-GFP-NLS contains EGFP fused to a nuclear localization signal driven by a cytomegalovirus promoter that we stably transfected into the parental cell line.

Clamp probe design and synthesis. Clamp probes are 150 nt long (15mer left RNA binding arm, 10 nt left adaptor, 100mer backbone, 10 nt right adaptor, 15mer right RNA binding arm). RNAs are targeted by probe sets containing one or more Clamp probes, each targeting a 30-nt region of RNA (two adjacent 15mer binding arms). We chose binding regions with approximately 40% G+C content as well as minimal repetitive regions using our probe design pipeline (source code available at <https://flintbox.com/public/project/50547/>) and instructions for use are available in the **Supplementary Protocol**. We designed backbones so as to minimize predicted secondary structure (using mFold; <http://unafold.rna.albany.edu/?q=mfold>). We ordered modified DNA oligonucleotides from Integrated DNA Technologies (IDT) as standard DNA oligonucleotides with modifications (5'-phosphate on the backbone, 3'-azide and 5'-phosphate for the right arm and 5'-hexynyl for the left arm). Strands were resuspended in nuclease-free water, at a working stock concentration of 400 μ M. The left arm (30 μ M), backbone (20 μ M) and right arm (30 μ M) are brought together using adaptor probes (30 μ M each) and denatured at 70 °C for 3 min before being enzymatically ligated using 600 U of T7 DNA ligase (New England BioLabs) for a minimum of 1 h at room temperature. Following ligation, the probes were purified using Monarch purification columns according to the manufacturer's instructions (New England Biolabs) and eluted in four times the starting volume to make the working dilution. For a schematic protocol and probe sequences, see **Supplementary Figure 1** and **Supplementary Table 1**.

ClampFISH procedure on cultured cells. We grew cells on glass coverslips until ~70% confluent. We washed the cells twice with PBS and then fixed them for 10 min with 4% formaldehyde in PBS at room temperature. We aspirated off the formaldehyde and rinsed twice with PBS before adding 70% ethanol for storage at 4 °C. We incubated our cells for at least 4 h at 37 °C in hybridization buffer (10% dextran sulfate, 2 \times SSC, 20% formamide) and 0.5 μ L of the working dilution of the primary ClampFISH probe. We performed two washes in wash buffer (2 \times SSC, 10% formamide), each consisting of a 30-min incubation at 37 °C. We then incubated the cells for at least 2 h at 37 °C in hybridization buffer (10% dextran sulfate, 2 \times SSC, 20% formamide) and 1 μ L of the working dilution of the secondary ClampFISH probe and repeated the washes. After the second wash, we performed the click reaction. A solution containing 75 μ M CuSO₄ premixed with 150 μ M BTAA ligand²⁰ (Jena Biosciences) and 2.5 mM sodium ascorbate (made fresh and added to solution immediately before use; Sigma) in 2 \times SSC was added to the samples, and these were then incubated for 30 min at 37 °C. The samples were then rinsed briefly with wash buffer, and then we continued cycling this protocol, alternating between secondary and tertiary ClampFISH probes until reaching the desired level of amplification. After the final wash, we rinsed once with 2 \times SSC/DAPI and once with antifade buffer (10 mM Tris (pH 8.0), 2 \times SSC, 1% w/v glucose). Finally, we mounted the sample for imaging in an antifade buffer with catalase (Sigma) and glucose oxidase² (Sigma) to prevent photobleaching. This method is described in more detail in the **Supplementary Protocol**.

ClampFISH for flow cytometry and sorting. ClampFISH for flow cytometry was performed as described above; however, the cells were kept in suspension. Wash buffer and 2 \times SSC were supplemented with 0.25% Triton-X, and the clampFISH hybridization buffer was supplemented with the following blocking reagents: 1 μ g/ μ L yeast tRNA (Invitrogen), 0.02% w/v bovine serum albumin, 100 ng/ μ L sonicated salmon sperm DNA (Agilent). We sorted on *NEAT1* and *HIST1H4E* RNA abundance using a FACSJazz (BD Biosciences) with a 640 nm excitation laser and 660/20 nm emission detector.

ClampFISH for expansion microscopy. Acryloyl-X, SEM 6-(6-(acryloyl)amino)hexanoic acid, succinimidyl ester, here abbreviated AcX; Thermo-Fisher) was

resuspended in anhydrous DMSO at a concentration of 10 mg/mL, aliquoted and stored frozen in a desiccated environment. Label-IT amine modifying reagent (Mirus Bio, LLC) was resuspended in the provided Mirus reconstitution solution at 1 mg/ml and stored frozen in a desiccated environment. To prepare LabelX, 10 μ L of AcX (10 mg/mL) was reacted with 100 μ L of Label-IT amine modifying reagent (1 mg/mL) overnight at room temperature with shaking. LabelX was subsequently stored frozen (-20 °C) in a desiccated environment until use.

Fixed cells were washed twice with PBS and incubated with LabelX diluted to 0.002 mg/mL in MOPS buffer (20 mM MOPS, pH 7.7) at 37 °C for 6 h, followed by two washes with PBS. Monomer solution (PBS, 2 M NaCl, 8.625% (w/w) sodium acrylate, 2.5% (w/w) acrylamide, 0.15% (w/w) *N,N'*-methylenebisacrylamide) was mixed, frozen in aliquots, and thawed before use. Prior to embedding, monomer solution was cooled to 4 °C to prevent premature gelation. Concentrated stocks (10% w/w) of ammonium persulfate initiator and tetramethylethylenediamine accelerator were added to the monomer solution up to 0.2% (w/w) each. One hundred microliters of gel solution specimens were added to each well of a Lab Tek 8 chambered coverslip and transferred to a humidified 37 °C incubator for 2 h.

Proteinase K (New England BioLabs) was diluted 1:100 to 8 units/mL in digestion buffer (50 mM Tris, pH 8, 1 mM EDTA, 0.5% Triton X-100, 0.8 M guanidine HCl) and applied directly to gels in at least ten times volume excess. The gels were then incubated in digestion buffer for at least 12 h. They were then incubated with wash buffer (10% formamide, 2 \times SSC) for 2 h at room temperature and hybridized with RNA FISH probes in hybridization buffer (10% formamide, 10% dextran sulfate, 2 \times SSC) overnight at 37 °C. Following hybridization, samples were washed twice with wash buffer, 30 min per wash, and washed four times with water, 1 h per wash, for expansion. Samples were imaged in water with 0.1 μ g/mL DAPI.

ClampFISH for mouse tissues. All studies were carried out under a protocol approved by the Institutional Animal Care And Use Committee at the University of Pennsylvania. Kidneys were collected from 4-d-old C57BL/6J mice. Dissected tissues were embedded in OCT, then flash frozen using liquid nitrogen. Tissue sections 5 μ m thick were cut at -20 °C and mounted on charged slides. Slides were washed briefly in PBS, then immersed in 4% paraformaldehyde for 10 min at room temperature. Following fixation, the slides were transferred to 70% ethanol for permeabilization for at least 12 h, or for long-term storage. To begin the clampFISH procedure, slides were transferred to wash buffer for 3 min to equilibrate and then 500 μ L of 8% SDS was added to the top of the flat slide for 1 min for tissue clearing. Samples were transferred to wash buffer, and the normal clampFISH procedure was used.

ClampFISH for multiplexing. Primary clampFISH probes for multiple targets (each with a different backbone series) are hybridized and washed at the same time. Each subsequent round is performed together using the respective secondary and tertiary probes, which are colorless. After the terminal round, samples are washed with 10% formamide, 2 \times SSC, then hybridized with RNA FISH probes in hybridization buffer (10% formamide, 10% dextran sulfate, 2 \times SSC) overnight at 37 °C. Following hybridization, samples were washed twice with wash buffer, 20 min per wash, then counterstained with DAPI nuclear stain and prepared for imaging.

DNA clampFISH on cultured cells. Probe design is performed the same as with RNA targets, but with 30mer left and right arms. We grew cells on glass coverslips until ~70% confluent. We washed the cells twice with PBS and then fixed them for 10 min with 4% formaldehyde in PBS at room temperature. We aspirated off the formaldehyde and rinsed twice with PBS before adding 70% ethanol for storage at 4 °C. We washed the cells twice for 5 min in PBS, then permeabilized the cells for 15 min at room temperature with PBS supplemented with 0.5% Triton X-100. We washed the cells twice with PBS, then treated the cells with 0.1 M HCl for 5 min. We washed the cells twice with 2 \times SSC, then treated with an optional incubation of 25 μ g/ml RNase A for 30 min at 37 °C. Cells were washed twice with 2 \times SSC and then equilibrated with 50% formamide in 2 \times SSC for 30 min. Liquid was aspirated and cells were denatured using 70% formamide, 2 \times SSC on a hot plate at 78 °C for 4.5 min. We incubated our cells for at least 4 h at 37 °C in hybridization buffer

(10% dextran sulfate, 2× SSC, 50% formamide) and 0.5 μL of the working dilution of the primary DNA clampFISH probe. Washes and subsequent rounds of clampFISH were done using the standard clampFISH procedure.

Comparison of amplification methods. *GFP* mRNA clampFISH was performed to round 6 according to the protocol reported above on WM983b-GFP and WM983b cells. These probes were Cy5 labeled, and signal intensity was compared to a corresponding single-molecule FISH probe set targeting *GFP* mRNA that was also labeled with Cy5. *GFP* mRNA was also detected using RNAscope technology according to the manufacturer's protocol (ACDbio). These probes were Atto 647 labeled, and signal intensity was compared to a corresponding single-molecule FISH probe set targeting *GFP* mRNA that was also labeled with Atto 647. *GFP* mRNA was also detected using hybridization chain reaction technology according to the manufacturer's protocol (Molecular Instruments). These probes were Alexa 647 labeled, and signal intensity was compared to a corresponding single-molecule FISH probe set targeting *GFP* mRNA that was also labeled with Alexa 647.

Imaging. We imaged each samples on a Nikon Ti-E inverted fluorescence microscope with a cooled CCD camera (Andor iKon 934). For 100× imaging, we acquired z-stacks (0.3 μm spacing between stacks) of stained cells. The filter sets we used were 31000v2 (Chroma), 41028 (Chroma), SP102v1 (Chroma), 17 SP104v2 (Chroma) and SP105 (Chroma) for DAPI, Atto 488, Cy3, Atto 647N/Cy5 and Atto 700, respectively. A custom filter set was used for Alexa 594 (Omega). We varied exposure times depending on the dyes and degree of amplification used. Typically, ClampFISH was imaged with an exposure of 300 ms and single-molecule RNA FISH with an exposure of 2–3 s.

Image analysis. We first segmented and thresholded images using a custom MATLAB software suite (downloadable at <https://bitbucket.org/arjunrajlaboratory/rajlabimagnetools/wiki/Home>). Segmentation of cells was done manually by drawing a boundary around non-overlapping cells. Unless otherwise specified, we called clampFISH and single-molecule RNA FISH spots using

the previously described algorithm in rajlabimagnetools (<https://bitbucket.org/arjunrajlaboratory/rajlabimagnetools/wiki/Home>).

Colocalization analysis. We performed spot colocalization analysis as previously described²⁹. Briefly, after initial spot calling, the algorithm used Gaussian fitting to refine spot localization estimates and then a two-stage algorithm incorporating chromatic aberration correction to identify pairs of spots colocalizing across two channels.

Expansion-FISH. We manually segmented cells as described above. We performed spot calling using the modified expansion spot-calling processor in rajlabimagnetools, as previously described.

Statistical analysis. All experiments were performed in multiple, independent experiments, as indicated in the figure legends. All statistics and tests are described fully in the text or figure legend. Error bars throughout represent s.e.m. unless otherwise specified.

Code availability. Scripts for all analyses presented in this paper, including all data extraction, processing, and graphing steps are freely accessible at https://www.dropbox.com/sh/b2mv4o9wmzicqv/AABARZsKtD1TQKMseoG_LnyWa?dl=0. Our image analysis software is available at <https://bitbucket.org/arjunrajlaboratory/rajlabimagnetools/wiki/Home>, changeset 6aa67c3b68c8dd5599fed681e1a21ec674464c65.

Reporting Summary. Further information on experimental design and reagents is available in the **Nature Research Reporting Summary** linked to this article.

Data availability. All raw and processed data used to generate figures and representative images presented in this paper are available at https://www.dropbox.com/sh/b2mv4o9wmzicqv/AABARZsKtD1TQKMseoG_LnyWa?dl=0.

29. Mellis, I.A., Gupte, R., Raj, A. & Rouhanifard, S.H. Visualizing adenosine-to-inosine RNA editing in single mammalian cells. *Nat. Methods* **14**, 801–804 10.1038/nmeth.4332 (2017).

Reporting Summary

Nature Research wishes to improve the reproducibility of the work that we publish. This form provides structure for consistency and transparency in reporting. For further information on Nature Research policies, see [Authors & Referees](#) and the [Editorial Policy Checklist](#).

Statistical parameters

When statistical analyses are reported, confirm that the following items are present in the relevant location (e.g. figure legend, table legend, main text, or Methods section).

n/a | Confirmed

- The exact sample size (n) for each experimental group/condition, given as a discrete number and unit of measurement
- An indication of whether measurements were taken from distinct samples or whether the same sample was measured repeatedly
- The statistical test(s) used AND whether they are one- or two-sided
Only common tests should be described solely by name; describe more complex techniques in the Methods section.
- A description of all covariates tested
- A description of any assumptions or corrections, such as tests of normality and adjustment for multiple comparisons
- A full description of the statistics including central tendency (e.g. means) or other basic estimates (e.g. regression coefficient) AND variation (e.g. standard deviation) or associated estimates of uncertainty (e.g. confidence intervals)
- For null hypothesis testing, the test statistic (e.g. F , t , r) with confidence intervals, effect sizes, degrees of freedom and P value noted
Give P values as exact values whenever suitable.
- For Bayesian analysis, information on the choice of priors and Markov chain Monte Carlo settings
- For hierarchical and complex designs, identification of the appropriate level for tests and full reporting of outcomes
- Estimates of effect sizes (e.g. Cohen's d , Pearson's r), indicating how they were calculated
- Clearly defined error bars
State explicitly what error bars represent (e.g. SD, SE, CI)

Our web collection on [statistics for biologists](#) may be useful.

Software and code

Policy information about [availability of computer code](#)

Data collection

All software used to count RNA spots is available at the following link:
<https://bitbucket.org/arjunrajlaboratory/rajlabimagetools/wiki/Home>
Briefly, we used custom Matlab software to segment the cells and assign thresholds to the spots, then analyzed the data using R Studio.
All of our code is available at the following link: https://www.dropbox.com/sh/b2mv4o9wmzcicqv/AABARZsKtD1TQKMseoG_LnyWa?dl=0

Data analysis

Scripts for all analyses presented in this paper, including all data extraction, processing, and graphing steps are freely accessible at the following url:
https://www.dropbox.com/sh/b2mv4o9wmzcicqv/AABARZsKtD1TQKMseoG_LnyWa?dl=0. Our image analysis software is available here:
<https://bitbucket.org/arjunrajlaboratory/rajlabimagetools/wiki/Home>, changeset 6aa67c3b68c8dd5599fed681e1a21ec674464c65. All raw and processed data used to generate figures and representative images presented in this paper are available at the following url:
https://www.dropbox.com/sh/b2mv4o9wmzcicqv/AABARZsKtD1TQKMseoG_LnyWa?dl=0

For manuscripts utilizing custom algorithms or software that are central to the research but not yet described in published literature, software must be made available to editors/reviewers upon request. We strongly encourage code deposition in a community repository (e.g. GitHub). See the Nature Research [guidelines for submitting code & software](#) for further information.

Data

Policy information about [availability of data](#)

All manuscripts must include a [data availability statement](#). This statement should provide the following information, where applicable:

- Accession codes, unique identifiers, or web links for publicly available datasets
- A list of figures that have associated raw data
- A description of any restrictions on data availability

All raw and processed data used to generate figures and representative images presented in this paper are available at the following url: https://www.dropbox.com/sh/b2mv4o9wmzcicqv/AABARZsKtD1TQKMseoG_LnyWa?dl=0.

Field-specific reporting

Please select the best fit for your research. If you are not sure, read the appropriate sections before making your selection.

Life sciences Behavioural & social sciences Ecological, evolutionary & environmental sciences

For a reference copy of the document with all sections, see [nature.com/authors/policies/ReportingSummary-flat.pdf](https://www.nature.com/authors/policies/ReportingSummary-flat.pdf)

Life sciences study design

All studies must disclose on these points even when the disclosure is negative.

Sample size	No sample-size calculation was performed. Sample sizes were selected by screening thousands of RNAs per experiment across many cells in a minimum of 2 independent experiments to show a fair distribution of the patterns observed
Data exclusions	No data were excluded from the analysis because all attempts at replication were successful.
Replication	All attempts at replication were successful. Each result in this manuscript has a minimum of 2 independent experiments.
Randomization	Samples were allocated into experimental groups based on individual treatments performed.
Blinding	Blinding was not relevant to this study

Reporting for specific materials, systems and methods

Materials & experimental systems

n/a	Involvement in the study
<input checked="" type="checkbox"/>	<input type="checkbox"/> Unique biological materials
<input checked="" type="checkbox"/>	<input type="checkbox"/> Antibodies
<input type="checkbox"/>	<input checked="" type="checkbox"/> Eukaryotic cell lines
<input checked="" type="checkbox"/>	<input type="checkbox"/> Palaeontology
<input type="checkbox"/>	<input checked="" type="checkbox"/> Animals and other organisms
<input checked="" type="checkbox"/>	<input type="checkbox"/> Human research participants

Methods

n/a	Involvement in the study
<input checked="" type="checkbox"/>	<input type="checkbox"/> ChIP-seq
<input type="checkbox"/>	<input checked="" type="checkbox"/> Flow cytometry
<input checked="" type="checkbox"/>	<input type="checkbox"/> MRI-based neuroimaging

Eukaryotic cell lines

Policy information about [cell lines](#)

Cell line source(s)	WM983b cells-Gift from Meenhard Herlyn's lab at the Wistar Institute MDA-MB-231 cells-ATCC HeLa cells-ATCC
Authentication	Short tandem repeat DNA profiling
Mycoplasma contamination	All cell lines tested negative for mycoplasma contamination.

Commonly misidentified lines
(See [ICLAC](#) register)

No commonly misidentified cell lines were used in this study.

Animals and other organisms

Policy information about [studies involving animals](#); [ARRIVE guidelines](#) recommended for reporting animal research

Laboratory animals

Kidneys were harvested from 4 day old, male C57BL/6J mice

Wild animals

No wild animals were used in this study.

Field-collected samples

This study did not involve field-collected samples.

Flow Cytometry

Plots

Confirm that:

- The axis labels state the marker and fluorochrome used (e.g. CD4-FITC).
- The axis scales are clearly visible. Include numbers along axes only for bottom left plot of group (a 'group' is an analysis of identical markers).
- All plots are contour plots with outliers or pseudocolor plots.
- A numerical value for number of cells or percentage (with statistics) is provided.

Methodology

Sample preparation

ClampFISH for flow cytometry was performed as described above however the cells were kept in suspension. Wash buffer and 2X SSC were supplemented with 0.25% Triton-X, and the clampFISH hybridization buffer was supplemented with the following blocking reagents: 1µg/µl yeast tRNA (Invitrogen), 0.02% w/v bovine serum albumin, 100ng/µl sonicated salmon sperm DNA (Agilent)

Instrument

FACSJazz (BD Biosciences)

Software

FlowJo

Cell population abundance

For separating based on GFP mRNA expression, we used the expression of GFP protein to determine abundance of each population.

Gating strategy

For separating based on GFP mRNA expression, we used the expression of GFP protein to gate GFP positive and negative cells. For gating endogenous targets, we used samples that were treated with clampFISH amplifiers, but no primary probe to define the negative cells and determine where positive signal began. We then gated and sorted the upper 10% and lower 10% of the populations.

- Tick this box to confirm that a figure exemplifying the gating strategy is provided in the Supplementary Information.